Measurement of cluster reorganization by time-resolved photoelectron spectroscopy

Jack A. Syage
The Aerospace Corporation, P.O. Box 92957/M5-754, Los Angeles, CA 90009, USA

Received 6 October 1992; in final form 6 November 1992

An excited-state proton transfer was initiated in the molecule phenol seeded in a solvent cluster of $(NH_3)_n$ and the subsequent reorganization of the solvent about the proton measured by time-resolved photoelectron spectroscopy. A shift in the broad photoelectron band on a timescale of 300 ps is attributed to a changing Franck–Condon distribution for ionization arising from reorganization of the solvent geometry.

1. Introduction

The rearrangement of a solvent structure about a reactive site (i.e. "solvation") is one of the most basic and important events in chemistry and has occupied the attention of chemists for decades. In this Letter, we describe a new method of measuring cluster reorganization (as a model of solvent relaxation) using time-resolved photoelectron spectroscopy. In the example given here, the cluster rearrangement is initiated by an excited-state proton transfer (ESPT) reaction from the S_1 state of phenol to a surrounding $(NH_3)_n$ solvent cluster [1,2]. The importance of measuring reactivity and solvent reorganization in clusters is the opportunity to relate chemical properties to specific solvent compositions, size, and structure, with well-defined energy. Condensed-phase studies measure an average of many possible solvent core environments, whereas cluster studies measure specific solvent environments. Recent cluster studies have shown that small changes in solvent properties can have dramatic effect on chemical reactivity [1–7].

Time-dependent spectral shifts in emission bands have been used to measure solvent relaxation in condensed phase. In these experiments, the relaxation dynamics are generally related by the correlation function

$$C(t)=\frac{\nu(t)-\nu(\infty)}{\nu(0)-\nu(\infty)}, \qquad (1)$$

where $\nu(t)$, $\nu(0)$, and $\nu(\infty)$ are the emission maxima at time t, $t=0$, and $t=\infty$, respectively [8–10]. $C(t)$ is predicted to decay exponentially in a pure Debye solvent with a longitudinal relaxation time constant τ_L. It is reasonable to expect that time-dependent photoelectron spectroscopy should be sensitive to similar structural dynamics in clusters.

This Letter also describes a new method in molecular beam time-of-flight (TOF) photoelectron spectroscopy. The device incorporates a paraboloidal electrostatic reflector (PER) to significantly increase the electron collection efficiency compared to conventional TOF spectrometers based on line-of-sight electron detection [11,12].

2. Experimental

A schematic of the photoelectron spectrometer is shown in fig. 1. The PER consists of two paraboloidal grid forms, separated by 1 mm at the apex, and biased to create a -5 V reflecting field for electrons. A skimmed molecular beam enters the PER through a hole in the apex and is crossed by a laser that enters and exists through two holes in the side. The intersection takes place at the focal point of the PER. All

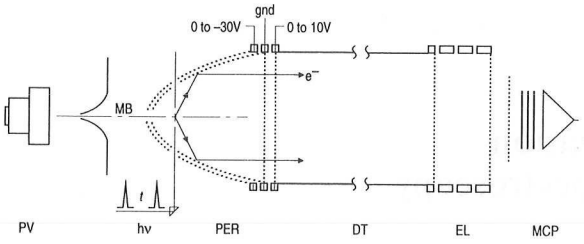

Fig. 1. Schematic off the paraboloidal electrostatic reflector (PER) used in the TOF photoelectron spectrometer. Terms are defined as follows: PV – pulsed valve; $h\nu$ – pump–probe pulses of delay time t; DT – drift tube; EL – einsel lens; MCP – microchannel plate detector.

reflected electrons become collimated and travel the same path length toward the detector. The drift tube is 1 m long. A twentyfold enhancement is observed for reflected electrons versus direct electrons. The direct electrons are currently unblocked and arrive at the detector about 2% sooner than reflected electrons of the same energy. The volume encompassed by the inner paraboloid and flat grid is maintained at zero field. Electrons are accelerated into the drift tube to enhance detection efficiency, particularly at low energy. Energy-resolved and time-resolved spectra were recorded using 1 and 5 V acceleration, respectively. Spectra were not corrected for the decreasing detection efficiency with decreasing electron energy.

An einsel-lens assembly at the end of the 9 cm diam drift tube is used to focus the electrons onto a 4 cm diam detector. The PER and drift tube are shielded from stray magnetic fields by two layers of μ-metal. The relatively strong signal levels permit the use of analog detection. Energy-resolved photoelectron spectra are recorded using a digital storage oscilloscope (350 MHz, 400 MHz sampling rate) and built-in signal averaging. Time-resolved spectra are recorded using a gated integrator set to collect signal from specific energy bands in the TOF photoelectron spectra. Although the cluster photoelectron spectra in fig. 2 are inherently broad, the instrument routinely achieves resolution of $\Delta E/E = 0.02$. A complete description of the apparatus will be published elsewhere [12].

The picosecond pump–probe arrangement has been described at length before [1,2]. Here we use 266 nm pump excitation and 532 nm two-photon

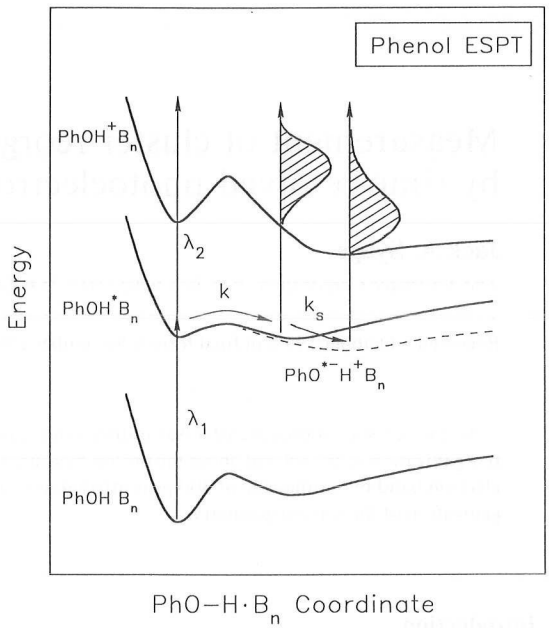

Fig. 2. Energy diagram $PhOH\cdot(NH_3)_n$ consistent with a cluster size of $n \approx 5$. ESPT proceeds along the O–H coordinate (rate constant k) and cluster reorganization occurs along solvent coordinates (rate constant k_s). The latter process is represented by an ion-pair minimum along the O–H coordinate that shifts to lower energy and longer bond distance. The shaded region shows how the photoelectron spectrum might change for solvent reorganization.

probe ionization of 18 and 25 ps nominal pulsewidths, respectively. The pump–probe delay time is scanned using a stepper-motor-controlled variable delay line. A phenol sample was placed in a temperature-controlled pulsed valve maintained at about 40°C. A mixture of 2% NH_3 in Ar was flowed into the pulsed valve at 30 psia pressure. These conditions were chosen to obtain a cluster size distribution, measured by mass spectrometry, that peaked at about $n=3$. The laser and pulsed valve are operated at 10 Hz.

3. Results

A potential energy diagram describing phenol ESPT and solvent reorganization is given in fig. 2. The excited-state reactant $PhOH^*...B_n$ ($B_n=(NH_3)_n$ in this work) is generated by 266 nm excitation,

which produces about 2500 cm^{-1} of vibrational energy. An ESPT reaction to give an excited ion-pair state occurs in about 60 ps for cluster sizes $n \geqslant 5$ [1]. The time dependence measured here is represented by the two-step process

$$PhOH^*...B_n \xrightarrow{k} [PhO^{*-}...H^+B_n]_{ur}$$

$$\xrightarrow{k_s} [PhO^{*-}...H^+B_n]_r ,$$

where the second step describes a solvent reorganization from an unrelaxed (ur subscript) to a relaxed (r subscript) solvent configuration. To a good approximation, the above steps are irreversible [1,2]. In fig. 2, we assume that the proton transfer (first step) proceeds primarily along the O–H coordinate. The change in the solvent coordinate, though not explicitly shown in fig. 2, is represented by a shift in the minima of the O–H ion pair potential to lower energy and longer O–H bond distance. This process represents further stabilization and positive charge delocalization by the relaxing solvent.

In previous work, we showed that the reactant and product excited-state clusters are detectable by mass spectrometry because ionization of reactant produces the $PhOH^+...(NH_3)_n$ ion series, whereas ionization of product leads to $PhO...H^+(NH_3)_n$ ions that dissociate to $H^+(NH_3)_m$ (cf. fig. 2b) [1,2] [#1]. The time dependence for the three species, denoted *a*, *b*, and *c*, respectively, is given by

$$a(t) = a(0)\exp(-kt) , \tag{2a}$$

$$b(t) = a(0)[1-\exp(-kt)]\exp(-k_s t) , \tag{2b}$$

$$c(t) = a(0)[1-\exp(-kt)] \times [1-\exp(-k_s t)] . \tag{2c}$$

This model was used to explain the dual time dependence for the build-up of the ion-pair signal given by $P^+(t) = i_b b(t) + i_c c(t)$ where i_b and i_c are ionization efficiencies [1]. We observed a $P^+(t)$ signal that increased with k_s indicating that $i_c > i_b$ (fig. 3 insert). This result is consistent with the premise that k_s is a measure of solvent relaxation. The argument given is that the proton-bound solvent relaxes to a configuration similar to the ion solvent structure (cf. fig. 2) giving rise to improved Franck–Condon factors for ionization. Bernstein and co-workers also observed a change in the ionization cross sections for ESPT in 1-naphthol-$(NH_3)_n$, which they attributed to solvent relaxation [6]. If these hypotheses are true, then a change in the solvent coordinate should lead to a shift in the Franck–Condon distribution for ionization that is detectable by time-resolved photoelectron spectroscopy. The shaded regions in fig. 2 show how the photoelectron energy distribution might change with solvent reorganization.

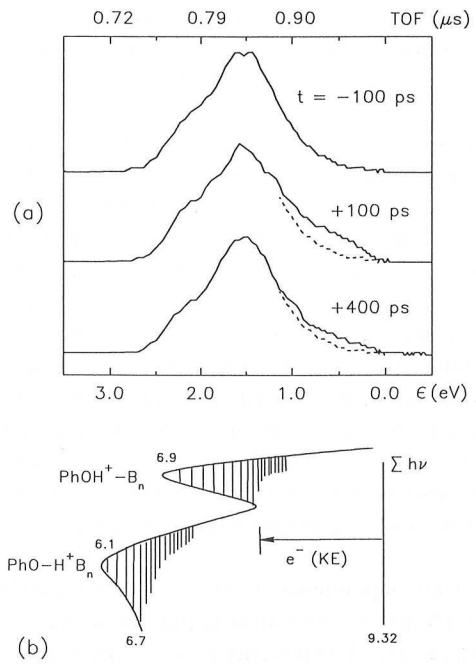

Fig. 3. (a) Photoelectron spectra as a function of pump–probe delay time *t*. The $t = -100$ ps spectrum is superimposed on the latter two spectra (dashed line) to emphasize the low-energy band. The abscissa shows electron time-of-flight, TOF, and corresponding energy, ϵ. (b) Estimated cluster ion potential energy curve along the O–H coordinate for $B_n = (NH_3)_5$ drawn to show relationship to photoelectron energies (labelled energy values in eV are from ref. [2]).

Photoelectron spectra from the reactant and product configurations above are presented in fig. 3. The spectrum for negative delay time ($t = -100$ ps) is identical to the 266 nm one-color spectrum and corresponds to ionization to the $PhOH^+...B_n$ complex. The high-energy limit of the spectrum agrees with

[#1] We use the term ionization in a general sense; the process of electron ejection from an ion pair is often referred to as photodetachment.

the reported ionization potential (IP) of 6.9 eV for the $n=4$ and 5 cluster sizes [13]. The smaller-cluster IP limits lie to lower energy and contribute to the broad peak. At positive delay times, a distinct two-color photoelectron band emerges at low energy. Because this band evolves within 100 ps of S_1 excitation, we attribute it to ionization from the ion-pair (proton-transfered complex) to the $PhO...H^+B_n$ complex. The band decays noticeably after 400 ps (fig. 3a). The current configuration of the photoelectron spectrometer does not allow mass determination. The cluster distribution contributing to the time-dependent part of the photoelectron signal is believed to be narrow because of the sharp threshold for reaction at $n=5$ and the use of a decreasing cluster size distribution. Mass spectra indicate that of the cluster sizes $n \geqslant 5$ about 80% fall in the range of $n=5$–7.

The time dependence for the low-energy and high-energy photoelectron bands is plotted in fig. 4. The low-energy band (high-energy ions) increases rapidly in intensity and then decays at a slower rate. The high-energy band (low-energy ions) shows a corresponding slow rate of increase. These results can be interpreted by a Franck–Condon distribution for ionization that evolves in time. The most likely explanation is that the solvent cluster configuration is changing. Other trends support this interpretation. The direction of the shift is from high-energy to low-energy ion excitation (red-shift transitions to the ion), as expected for solvent relaxation. The low-energy band decays to a plateau level rather than to the baseline suggesting a spectral shift that is less than the width of the band. The high-energy band should grow from a similar non-zero baseline at $t<0$, however, this level is obscured by the one-color background signal.

Other explanations for the observed time-dependences can be ruled out. A possible culprit is evaporation; however our past [1] and present studies show that evaporation (1) occurs on a many nanosecond timescale, (2) cannot explain the *increase* in the total product ion signal (fig. 4, insert), and (3) would give a high-energy to low-energy shift in the photoelectron spectrum, opposite to what is observed here for solvent reorganization. Another possibility is that the low-energy electron band is due to one-photon ionization, which is energetically allowed, though maybe not Franck–Condon favored (fig. 3b) [2]. The intensity ratio for one- and two-photon ionization would still evolve in time due to solvent reorganization, but the expected shift in energy by this mechanism is opposite to what is observed here. Also, our previous work shows that the $PhO...H^+(NH_3)_{n>4}$ complex dissociates to $H^+(NH_3)_m$ completely for 532 nm ionization, but only partially for 355 nm ionization, indicating that the former is a two-photon process [1,2]. The possibility of an ion-pair dissociation to $PhO^- + H^+B_n$ was ruled out in our previous work using negative ion mass spectrometry [1]. The nature of the two-photon probe ionization mechanism remains unclear and may involve an intermediate state. However, this uncertainty does not change the interpretation that the time-evolving photoelectron spectrum reflects dynamics in the excited neutral state and the best explanation is that geometry change is causing a shift in the Franck–Condon distribution.

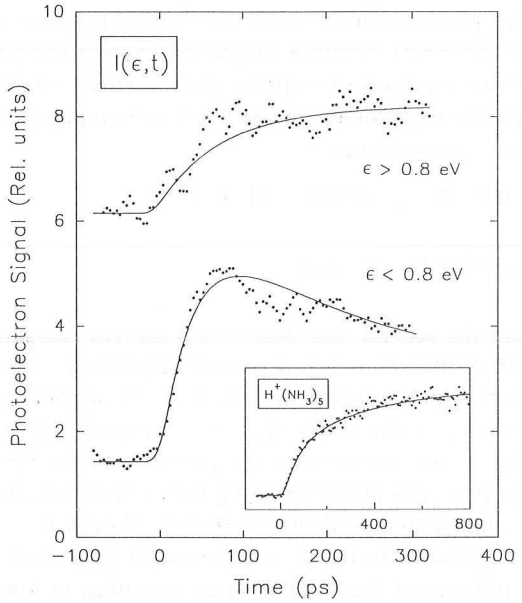

Fig. 4. Time-dependence of low-energy ($0.8>\epsilon>0$ eV) and high-energy ($2.6>\epsilon>0.8$ eV) photoelectron bands (using 140 ns gates under conditions of fig. 2a). Fitted curves were calculated for rate constants $k=(50\ \text{ps})^{-1}$ and $k_2=(300\ \text{ps})^{-1}$ and spectral parameters $\epsilon_0=0.7$ eV, $\sigma=0.6$ eV, and $\lambda_S=0.5$ eV. Calculated decay and formation curves correspond to $\epsilon=0.5$ eV and 1.2 eV, respectively. Insert shows time dependence for total product ion yield (from ref. [1]) fitted to values of $k=(65\ \text{ps})^{-1}$ and $k_s=(300\ \text{ps})^{-1}$.

4. Discussion

We develop a simple model for describing the time dependence of the photoelectron spectrum by assuming that the Franck–Condon photoelectron band is a Gaussian of width σ and shifts by λ_S due to solvent reorganization. The time dependence as a function of photoelectron energy ϵ is given by

$$g(\epsilon, t)=\exp\left(-\frac{[(\epsilon_0+\lambda_S-\epsilon)-\lambda_S\rho(t)]^2}{\sigma^2}\right), \quad (3)$$

where ϵ_0 is the energy of the band maximum at $t=0$ (unrelaxed spectrum) and $\rho(t)$ is the time dependence for the band maximum. The function $\rho(t)$, which is equivalent to $C(t)$ in eq. (1) in this simple model, is a measure of cluster relaxation along the solvent coordinate. We define $\rho(t)$ as a decaying function ($\exp(-k_s t)$ hereafter) so that the band maximum $\epsilon_0+\lambda_S[1-\rho(t)]$ is ϵ_0 at $t=0$ and $\epsilon_0+\lambda_S$ at $t=\infty$. For positive λ_S, the photoelectron band shifts to higher energy (i.e. lower ion energy), corresponding to a red-shift in terms of the product-state to ion-state transition energy. This is the predicted direction of change for a solvent cluster that undergoes a change in configuration that better resembles the equilibrium geometry of the cluster ion. Some of the assumptions of our simple model include describing the solvent modes classically by a single reorganization parameter λ_S, ignoring internal modes in the Franck–Condon distribution, assuming a constant width parameter σ with time, and assuming a constant integrated photoelectron band intensity with time.

To illustrate the expected time dependence as a function of photoelectron energy, we consider the simple case of $\epsilon=\epsilon_0$ and $\epsilon=\epsilon_0+\lambda_S=\epsilon_\infty$. From eq. (3), we obtain

$$g(\epsilon_0, t)=\exp\left(-\frac{\lambda_S^2}{\sigma^2}[1-\exp(-k_s t)]^2\right), \quad (4a)$$

$$g(\epsilon_\infty, t)=\exp\left(-\frac{\lambda_S^2}{\sigma^2}\exp(-2k_s t)\right). \quad (4b)$$

These expressions show that $g(\epsilon_0, t)$ decreases with time and $g(\epsilon_\infty, t)$ increases with time. In the limits of $t=0$ and $t=\infty$, one obtains

$$g(\epsilon_0, 0)=1, \quad g(\epsilon_0, \infty)=\exp\left(-\frac{\lambda_S^2}{\sigma^2}\right), \quad (5a)$$

$$g(\epsilon_\infty, 0)=\exp\left(-\frac{\lambda_S^2}{\sigma^2}\right), \quad g(\epsilon_\infty, \infty)=1\,. \quad (5b)$$

The function $g(\epsilon, t)$ is sensitive to the values of ϵ, the spectral parameters λ_S and σ, and the functional form of $\rho(t)$. Accurate determination of each of these properties can be obtained by recording a series of time-resolved measurements over narrow electron energy bands or by recording the evolving photoelectron band over narrow time intervals.

The time dependences observed in fig. 4 show the qualitative behavior described by eqs. (3)–(5). The calculated curves through the points were fitted by the expression

$$I(\epsilon, t)=\int_{-\infty}^{\infty} f(t-t')[1-\exp(-kt')]g(\epsilon, t')\,\mathrm{d}t', \quad (6)$$

which includes the instrument time response and ESPT product formation kinetics. Because the timescale for these functions is much shorter than for solvent reorganization, the time dependence for the observed signal $I(\epsilon, t)$ is nearly equivalent to $g(\epsilon, t)$.

The quality of the fits in fig. 4 is not quantitative, but reasonable considering the simplicity of the working model and the current limitations of the experiment. The approximations in the model that affect the fits include the assumptions of (1) a single exponential function for $\rho(t)$, (2) Gaussian photoelectron bands, and (3) band widths and integrated intensities (i.e. total ion yield) that are invariant with time. The experimental uncertainties that currently prevent a unique fit include (1) insufficient data on the photoelectron band widths and band maxima due to varying kinetic energy detection efficiency and overlap with the one-color signal, and (2) the recording of time-resolved spectra over a broad electron energy width. Spectral parameters used in the calculated curves were estimated from higher resolution spectra and are listed in the caption to fig. 4. The rate constants $k=(50\ \mathrm{ps})^{-1}$ and $k_s=(300\ \mathrm{ps})^{-1}$, used to fit the data, are in excellent agreement with the time-resolved mass spectrometry results (fig. 4 insert).

The measured rate constants k and k_s can be interpreted in context of condensed-phase solvation. It is generally assumed that electron transfer (ET) and proton transfer (PT) tunneling rates are limited by solvent relaxation such that $k \leqslant \tau_L^{-1}$ (i.e. dynamic solvent effect; $k \approx \tau_L^{-1}$ for barrierless process). In hydrogen-bonding solvents it is common to refer to three Debye (dielectric response) relaxation times due to large amplitude aggregate motions involving hydrogen-bonding dynamics (τ_{D1}), molecular rotation or reorientation (τ_{D2}), and internal rotation (τ_{D3}, more relevant to alcohols than to NH_3) [8–10]. The lowest frequency motions are known to dominate the dielectric response of a solvent and hence τ_{D1} is usually associated with τ_L. Simple theories then predict that the rates of ET and PT should not exceed τ_L^{-1}. Our results, however, show that the rate constant k for ESPT is substantially faster than k_s in these clusters. Similar rate disparities have been observed in the condensed phase [8–10], and recent theories now cite the importance of higher frequency solvent fluctuations and solute intramolecular modes to chemical rates [14]. A plausible interpretation of our cluster dynamics is that ESPT is facilitated by reorientational solvent fluctuations ($k \approx \tau_{D2}^{-1}$) or intramolecular solute dynamics and that k_s, which measures geometry changes, is associated with τ_{D1}.

The point of this brief discussion is to illustrate that solvent dynamics can be interpreted in clusters and that time-resolved mass and electron spectroscopy of clusters offers several unique capabilities, including (1) unequivocal separation of the chemical dynamics from solvent dynamics, (2) separation of solvent–core effects from surrounding solvent shells, (3) ability to measure distinct solvent environments rather than averaged solvent environments in condensed-phase samples, (4) opportunities to study vibrational and even quantum-mechanical effects (solvent modes, tunneling, etc.). Finally, these techniques are applicable to studying other molecular-level dynamical properties of matter on a molecular level such as structural isomerization in clusters [15].

In summary, we have introduced time-resolved photoelectron spectroscopy to the study of cluster dynamics and made a direct measure of the reorganization of a solvent structure perturbed by a chemical reaction.

Acknowledgement

This work was funded by the Aerospace Sponsored Research program.

References

[1] J.A. Syage and J. Steadman, J. Chem. Phys. 95 (1991) 2497; J. Steadman and J.A. Syage, J. Chem. Phys. 92 (1990) 4630.
[2] J. Steadman and J.A. Syage, J. Am. Chem. Soc. 113 (1991) 6786; J. Phys. Chem. 95 (1991) 10326.
[3] J.J. Breen, W.-B. Tzeng, K. Kilgore, R.G. Keesee and A.W. Castleman Jr., J. Chem. Phys. 90 (1989) 19.
[4] O. Cheshnovsky and S. Leutwyler, Chem. Phys. Letters 121 (1985) 1;
T. Droz, R. Knochenmuss and S. Leutwyler, J. Chem. Phys. 93 (1990) 4520.
[5] J.J. Breen, L.W. Peng, D.M. Willberg, A. Heikal, P. Cong and A.H. Zewail, J. Chem. Phys. 92 (1990) 805;
D.M. Willberg, M. Gutman, J.J. Breen and A.H. Zewail, J. Chem. Phys. 96 (1992) 198.
[6] M.F. Hineman, G.A. Bruker, D.F. Kelley and E.R. Bernstein, J. Chem. Phys. 97 (1992) 3341.
[7] D. Ray, N.E. Levinger, J.M. Papanikolas and W.C. Lineberger, J. Chem. Phys. 91 (1989) 6533;
J.M. Papanikolas, J.R. Gord, N.E. Levinger, D. Ray, V. Vorsa and W.C. Lineberger, J. Phys. Chem. 95 (1991) 8028.
[8] J.D. Simon, Accounts Chem. Res. 21 (1988) 128;
S.-G. Su and J.D. Simon, J. Chem. Phys. 89 (1988) 908.
[9] M. Maroncelli, J. MacInnis and G.R. Fleming, Science 243 (1989) 1674;
G. Rothenberger, D.K. Negus and R.M. Hochstrasser, J. Chem. Phys. 79 (1983) 5360.
[10] P.F. Barbara, G.C. Walker and T.P. Smith, Science 256 (1992) 975;
W. Jarzeba, G.C. Walker, A.E. Johnson, M.A. Kahlow and P.F. Barbara, J. Phys. Chem. 92 (1988) 7039.
[11] D.J. Trevor, L.D. Van Woerkom and R.R. Freeman, Rev. Sci. Instr. 60 (1989) 1051;
G. Liu, J.J. Barton, C.C. Bahr and D.A. Shirley, Nucl. Instr. Meth. A 246 (1986) 504.
[12] J. Steadman and J.A. Syage, Rev. Sci. Instr., to be published; J.A. Syage and J. Steadman, J. Phys. Chem. 96 (1992), in press.
[13] D. Solgadi, C. Jouvet and A. Tramer, J. Phys. Chem. 92 (1988) 3313;
C. Jouvet, C. Lardeux-Dedonder, M. Richard-Viard, D. Solgadi and A. Tramer, J. Phys. Chem. 94 (1990) 5041.
[14] J.T. Hynes, J. Phys. Chem. 90 (1986) 3701;
H. Sumi and R. Marcus, J. Chem. Phys. 84 (1986) 4894.
[15] A. Heidenreich, J. Jortner and I. Oref, J. Chem. Phys. 97 (1992) 197.